# Density- and functional-driven errors in water clusters

Aaron D. Kaplan, <sup>1, 1</sup> Chandra Shahi, <sup>2, 2</sup> Raj K. Sah, <sup>3</sup> Pradeep Bhetwal, <sup>4</sup> and John P. Perdew<sup>2,3,‡</sup> 

1 Materials Project, Lawrence Berkeley National Laboratory, Berkeley, California 94720, USA

Department of Physics and Engineering Physics, Tulane University, New Orleans, LA 70118

Department of Physics, Temple University, Philadelphia, PA 19122

Department of Chemistry, Temple University, Philadelphia, PA 19122 (Dated: April 5, 2024)

Bolstered by recent calculations of exact functional-driven errors (FEs) and density-driven errors (DEs) of semi-local density functionals in the water dimer binding energy [Kanungo *et al.*, J. Phys. Chem. Lett. 15, 323 (2023)], we investigate *approximate* FEs and DEs in neutral water clusters containing up to 20 monomers, charged water clusters, and in alkali- and halide-water clusters. We show that SCAN makes substantially larger FEs for neutral water clusters than r<sup>2</sup>SCAN, while both make essentially the same DEs. Unlike the case for barrier heights, these FEs are small in a relative sense, and become large in an absolute sense only due to an increase in cluster size. SCAN@HF produces a cancellation of errors that makes it chemically accurate for predicting the absolute binding energies of water clusters. Likewise, adding a long-range dispersion correction to r<sup>2</sup>SCAN@HF, as in the composite method HF-r<sup>2</sup>SCAN-DC4, makes its FE more negative than in r<sup>2</sup>SCAN@HF, permitting a near-perfect cancellation of FE and DE. r<sup>2</sup>SCAN by itself (and even more so, r<sup>2</sup>SCAN evaluate on its 50% global hybrid density), is almost perfect for the energy differences between water hexamers, and thus probably also for liquid water away from the boiling point. Thus the accuracy of composite methods like SCAN@HF and HF-r<sup>2</sup>SCAN-DC4 is not due to the HF density being closer to the exact density, but to a compensation of errors from its greater degree of localization. We also give an argument for the approximate reliability of this unconventional error

cancellation for diverse molecular properties.

### I. INTRODUCTION

4

As density functional theory (DFT) is perhaps the most widely used theoretical framework for materials and chemical discovery, understanding the errors that density functional approximations (DFAs) make is critical to simulating electronic matter with experimentally-useful accuracy. In this work, which deals primarily with small gasphase water clusters, we take that threshold of chemical accuracy to be 1 kcal/mol in absolute error (about 43.36 meV). There are many possible sources of error in any density functional calculation, including purely numerical ones, and thus there are a few frameworks for studying these errors. DFAs that make small errors in water-cluster binding energies can be used for accurate simulations of water, a material of central importance to chemistry and biology.

Physically, the exact total energy is piecewise linear as a function of fractional electron number, often called the Perdew-Parr-Levy-Balduz (PPLB) theorem [1]. Semilocal approximations to the exchangecorrelation energy  $E_{\rm xc}$ , such as the local spin-density approximation (LSDA), generalized gradient approximation (GGA), and meta-GGA, are of the form

 $E_{xc}[n\uparrow,n\downarrow] = d^3re_{xc}(r). \tag{1}$ 

In LSDA, the exchange-correlation energy density  $e_{\rm xc}$  depends only on the spin densities  $n_1$  and  $n_4$ ; the GGA further depends on their gradients; and the meta-GGA further depends on the local kinetic energy spin-densities. As a function of fractional electron number N, the energy of a semilocal functional bends below the exact straightline segment [1]. This convexity leads to delocalization error, with non-integer electron numbers on separated fragments [1, 2]. Hartree-Fock (HF) theory, or its analogue in Kohn-Sham theory, the exchange-only approximation, tends to bend above the straight-line condition, called localization error [2].

In calculating the dissociation of molecular dimers, delocalization errors can cause a DFA to minimize with a spurious charge transfer, even in the limit of infinite separation [1, 2]. Explicit self-interaction corrections [3] to a DFA can eliminate this charge transfer. Thus selfinteraction errors are related to delocalization errors.

Because HF lowers the total energy by localizing the charge density on nuclear centers, it tends to correctly produce integer charges on isolated fragments in the dissociation limit. However, in water clusters in (meta)stable configurations, it was observed [4] that the HF density indeed produces a localizing transfer error, measured relative to an essentially exact density. The density from the strongly constrained and appropriately normed (SCAN) meta-GGA [5]

<sup>&</sup>lt;sup>1</sup> adkaplan@lbl.gov

<sup>&</sup>lt;sup>2</sup> schandra@temple.edu <sup>‡</sup> perdew@temple.edu

made errors that were comparable to those of HF in magnitude, but of opposite sign.

Similar patterns of charge transfer errors were recently noted in the transition states of reaction barriers [6].

An alternate framework [7] highlights the errors made in the approximate functional itself, and in its selfconsistent density. This density-corrected DFT, or DCDFT, [7–10] decomposes the total error  $\Delta E$  made by a DFA

$$\Delta E(DFA) = E_{DFA}[n_{DFA}] - E_{exact}[n_{exact}]$$
 (2)

into a functional-driven error (FE)

FE(DFA) = EDFA[nexact] - Eexact[nexact], and a density-driven error (DE)

$$DE(DFA) = E_{DFA}[n_{DFA}] - E_{DFA}[n_{exact}].$$
 (4)

DC DFT classifies calculations as normal, where  $|FE|\gg |DE|$ , and abnormal, where  $|FE|\lesssim |DE|$ . In abnormal cases, applying a density correction to a DFA will remove its density errors. Ideally, this would be non-selfconsistent evaluation on the exact density, but in practice, the density is usually that of HF. The HF density is usually more accurate than the DFA density in these cases, as has been shown for the binding energies and dissociation energies of halogenated and chalcogenated molecules [11]. Thus the converse is often assumed: When non-self-consistent application of a DFA to the HF density, called HF-DFT or DFA@HF, produces lower errors than the self-consistent DFA, a system is abnormal, and the HF density is more correct than the DFA's.

In practice, it is extremely difficult to find a corresponding Kohn-Sham system that yields the same density as a correlated wavefunction method. This is necessary in part because the Kohn-Sham auxiliary system relies upon a non-interacting kinetic energy term, which has no simple analogue in correlated wavefunction theory. This typically precludes evaluation of  $E_{\rm DFA}[n_{\rm exact}]$ .

However, the FE and DE are of obvious practical interest. Therefore, Ref. [6] recently developed a methodology for approximating these quantities using proxies for the exact density:

$$FE(DFA) \approx EDFA[n_{proxy}] - E_{exact}[n_{exact}]$$
 (5)

$$DE(DFA) \approx E_{DFA}[n_{DFA}] - E_{DFA}[n_{proxy}].$$
 (6)

For the data sets considered here and in Ref. [6], accurate values of  $E_{\rm exact}[n_{\rm exact}]$  are tabulated from correlatedwavefunction methods. Ref. [6] established that using only the proxy density or using both the proxy density and proxy energy {replacing  $E_{\rm exact}[n_{\rm exact}]$  by  $E_{\rm proxy}[n_{\rm proxy}]$  in Eq. (5)} gave qualitatively consistent analyses. However, using only the density (and not the energy) of the proxy minimizes the errors made by this approximation. Using these approximations for FE and DE, Ref. [6] found that  $|FE| \gg |DE|$  in reaction barrier heights, despite the well-documented fact

that HF-DFT significantly reduces the errors of DFAs in predicting toosmall barriers to chemical reactions.

For reaction barriers, the FEs and DEs of common DFAs tended to be negative [6] However, DE(DFA@HF) was typically positive and of much larger magnitude than DE(DFA). This suggested that the overly-local HF density produces a density over-correction for the barrier heights. A careful analysis of charge transfer errors in transition states showed that SCAN and HF made spurious charge transfers of similar magnitude but of opposite sign.

However, as this was the first work to present approximate FEs and DEs, there was no formal or statistical assurance that these values were meaningful. Subsequent work performed a direct inversion of the CCSD(T) density for the water dimer [12]. This work confirmed the accuracy of the approximate methods of Ref. [6] for a small, prototypical reaction barrier considered in Ref. [6]:  $H_2 + F \rightarrow H...H...F \rightarrow H + HF$ . When the density of the 50% global hybrid of r<sup>2</sup>SCAN, r<sup>2</sup>SCAN50, was used as a proxy for the exact density, the errors in the approximate FE and DE were small for the barrier heights and less than 0.1 kcal/mol for the water dimer. Doing this inversion for larger water clusters might not be sufficiently accurate, or even feasible, due to the larger number of electrons. Appendix Fig. 6 shows that the 50-100% global hybrids of r<sup>2</sup>SCAN predict water cluster BEs with average absolute errors below 1 kcal/mol; although the BE errors minimize for about 70% exact exchange, the r<sup>2</sup>SCAN70 density may be too localized to be a good proxy for the exact one.

Ref. [12] also proposed an explanation for the error cancellations, based on the observation that, in the presence of static nuclei, a semilocal functional becomes more accurate for a given density as that density becomes more localized. The present work continues the analysis of Refs. [6, 12] by performing approximate DC DFT analysis of water clusters. This work seeks to explain or understand the mechanisms by which the composite methods SCAN@HF [4, 13] and HF-r<sup>2</sup>SCAN-DC4 [14] achieve chemical accuracy in predicting the properties of gas-phase water clusters.

Section II details the computational methods used in this work, and Sec. III presents our findings for four sets of water clusters. In Sec. III, we carefully balance a discussion both of absolute errors and approximate functional- and density-driven errors to see how SCAN@HF and HF-r<sup>2</sup>SCAN-DC4 perform, and where they fall short.

# II. COMPUTATIONAL METHODS

Four data sets of water clusters are considered in this work: the benchmark energy and geometry database (BEGDB) neutral water cluster subset [15]; the WATER27 [16] set of 14 neutral, 5 protonated, 7 deprotonated, and one auto-ionized water cluster; and two sets of ion-water clusters  $M...(H_2O)_n$ , where  $M = \text{Li}^+$ ,  $\text{Na}^+$ ,  $\text{K}^+$ ,  $\text{F}^-$ ,  $\text{Cl}^-$ , or  $\text{Br}^-$ , and n = 1, 2. BEGDB

geometries, optimized at the RI-MP2/aug-cc-pVDZ level [17], were taken from their database. Reference energies for the BEGDB cohesive energies are taken from Ref. [18].

We use "platinum" standard values when available; gold standard values when platinum values are unavailable; and silver standard when neither higher-level values are available. WATER27 geometries and reference energies were taken from the GMTKN55 database [19]. For both the BEGDB and WATER27 sets, we used the aug-ccpVQZ [20] basis set. Last, for the alkali- and halidewater clusters, all reference energies and geometries were taken from Ref. [21]. As no aug-cc-pVQZ basis set for potassium exists, we use the comparable def2-QZVPPD [22-24] basis set for the alkali- and halide- clusters. No corrections for basis-set superposition errors were made. For the halide-water clusters, we find that computed binding energies are highly sensitive to the basis set. A comparison to binding energies computed previously in Ref. [21] shows that the basis set used there is insufficient to give an accurate description of the halide-water cluster binding energies. This likely indicates significant dispersion interactions in these clusters.

All calculations were performed with PySCF [25-27]. All systems were treated as spin-restricted, with (self-consistent) total energies converged below  $10^{-7}$  hartree, on the largest default integration grid (grid level 9). To approximate the exchange-correlation energy, we use only the stronglyconstrained and appropriately normed (SCAN) [5] metageneralized gradient approximation (meta-GGA), and its numerically-stable counterpart r2SCAN (regularized-restored SCAN) [28]. For the alkali- and halide-water clusters, we also analyze the errors made by the self-interaction corrected SCAN and r<sup>2</sup>SCAN. These calculations were done using the Fermi-Löwdin orbital self-interaction correction (FLOSIC) scheme in the NRLMOL-FLOSIC code [29]. All total energies in FLOSIC were converged to 10<sup>-7</sup> hartree, and all forces on Fermi-orbital descriptors (controlling the localization of the orbitals used in FLOSIC) were converged to  $5 \times 10^{-4}$ hartree/bohr.

### III. RESULTS AND DISCUSSION

## A. Neutral water clusters

We begin with the negative-definite binding energies (BEs) of the neutral water clusters in the BEGDB set, defined as

$$\Delta E_{\text{BE}} = E_{\text{opt}}((\text{H}_2\text{O})_k) - kE_{\text{opt}}(\text{H}_2\text{O}). \tag{7}$$

The subscript "opt" indicates that the optimized, or relaxed, geometry is used. This is in contrast to the interaction energy (IE)

$$\Delta E_{\text{IE}} = E_{\text{opt}}((\text{H2O})k) - XE_{\text{dist}(l)}(\text{H2O}), \tag{8}$$

i=1

which is the energy to break a cluster into its k distorted ("dist") monomers. The relaxation energy, or change in energy due to relaxation of a cluster's constituent monomers, is simply

$$\Delta E_{RE} = \Delta E_{IE} - \Delta E_{BE}$$

$$= kE_{opt}(H_2O) - XE_{dist(i)}(H_2O).$$

$$= 1$$

$$= (9)$$

Table I presents error statistics in these three quantities for SCAN and r<sup>2</sup>SCAN, both computed self-consistently and nonself-consistently at the Hartree-Fock (HF) density. SCAN@HF is uncannily accurate - yielding mean absolute deviations (MADs) well within the threshold of chemical accuracy, 1 kcal/mol. By comparison, SCAN's predictions of the BEs and IEs are quite inaccurate, both with MADs of about 5.5 kcal/mol. For the water clusters, SCAN and r<sup>2</sup>SCAN likely make an erroneous and spurious transfer of charge between neighboring monomers. For an isolated water monomer near equilibrium, such a spurious charge transfer is less likely. Thus, as SCAN and r2SCAN predict accurate REs, also found for SCAN in Ref. [4], they likely produce realistic densities and energies for the monomers. Appendix Fig. 6 shows that the RE MADs of the r<sup>2</sup>SCAN global hybrids r<sup>2</sup>SCANa rise almost linearly as a is increased from 0 (r<sup>2</sup>SCAN) to 1 (full exact exchange with r<sup>2</sup>SCAN correlation).

Although SCAN and r<sup>2</sup>SCAN perform nearly identically for simple, closed-shell systems, the BEGDB set highlights that pronounced differences between the two can occur. r<sup>2</sup>SCAN@HF shows no similar gain in accuracy over r<sup>2</sup>SCAN, which makes almost half the average absolute errors of SCAN for the BEs and IEs. To understand why, we compute approximate FEs and DEs using r<sup>2</sup>SCAN50 as a proxy for the exact density only. Table I also presents approximate mean FEs and DEs. Note that, consistent with Refs. [6, 12], we define

$$FE(DFA@HF) = FE(DFA)$$
 (10)

$$DE(DFA@HF) = EDFA[nHF] - EDFA[nexact].$$
 (11)

While SCAN makes large negative FEs,  $\sim -4.2$  kcal/mol on average, r<sup>2</sup>SCAN makes much smaller |FE|,  $\sim$ 

 $-1.8~\rm kcal/mol$  on average. Non-self-consistent evaluation of SCAN or r²SCAN on the HF density then induces a density-over-correction, increasing the DEs of SCAN@HF and r²SCAN@HF to about 4.7 kcal/mol from  $-1.4~\rm kcal/mol$ . This over-correction cancels the FE of SCAN nearly perfectly, but over-compensates r²SCAN's smaller FEs. The addition of a long-range D4 dispersion correction [30] (which depends only upon the molecular geometry and not the functional) in HF-r²SCAN-DC4 makes its FE more negative than in r²SCAN@HF, permitting a near-exact cancellation of FE and DE. Fig. 1 plots

the FEs and DEs of SCAN and  $r^2$ SCAN, both selfconsistent and @HF, for the individual BEGDB clusters. For all water clusters in the BEGDB set, the D4 dispersion correction, as tuned for HF- $r^2$ SCAN-DC4 [14] ( $s_6 = 1$ ,  $s_8 = -0.36$ ,  $a_1 = 0.23$ , and  $a_2 = 5.23$ ) yields a more negative dispersion correction for the k-mer than

because it has been observed that r<sup>2</sup>SCAN likely describes a lower fraction of the intermediate-range van der Waals interaction than SCAN [31]. This is consistent with the observation, also underpinning the theoretical motivation of the D-series dispersion corrections, that explicit inclusion of dispersion interactions should primarily change a functional's

	BE			IE			RE			
DFA	MD N	1AD MFE MI	DE	MD	MAD MFE MDE		MD	MAD MF	E MDE	
SCAN	-5.62	5.62 -4.18	-1.44	-5.56	5.56 -4.29	-1.28	0.05	0.06	-0.10	0.16
SCAN@HF	0.59	0.59 -4.18	4.77	0.12	0.23 -4.29	4.40	-0.47	0.4	7 -0.10	-0.37
r <sup>2</sup> SCAN	-3.19	3.19 -1.76	-1.43	-3.02	3.02 -1.74	-1.28	0.17	0.17	0.02	0.15
r <sup>2</sup> SCAN@HF	2.92	2.92 -1.76	4.68	2.57	2.57 -1.74	4.31	-0.35	0.35	0.02	-0.37
HF-r <sup>2</sup> SCAN-DC4 C	0.09	0.09 -4.59	4.68	-0.25	0.26 -4.56	4.31	-0.34	0.34	0.03	-0.37
r <sup>2</sup> SCAN50	-0.8	4 0.85		-4.08	4.08		-3.24	3.24		

TABLE I. Summary of error statistics of the BEGDB subset [15] of neutral water clusters. For the binding energies (BEs), interaction energies (IEs), and relaxation energies (REs), mean deviations (MDs) and mean absolute deviations (MADs) are presented. These are computed using Eqs. (7)–(9). Mean functional-driven errors (MFEs) and mean density-driven errors (MDEs) are computed using the 50% global hybrid of  $r^2$ SCAN as a proxy for the exact density. (The accuracy of the  $r^2$ SCAN50

BE seems to arise from an unexplained error cancellation between IE and RE.) All units are kcal/mol. By construction, MD = MFE + MDE. To compute FE and DE for HF- $r^2$ SCAN-DC4, we compute FE( $r^2$ SCAN-D4) and DE( $r^2$ SCAN-D4@HF), where the D4 correction uses the same parameters as in HF- $r^2$ SCAN-DC4. Practically, because D4 only depends upon the molecular geometry, we garnish the  $r^2$ SCAN total energies with the dispersion correction computed with HF- $r^2$ SCAN-DC4.

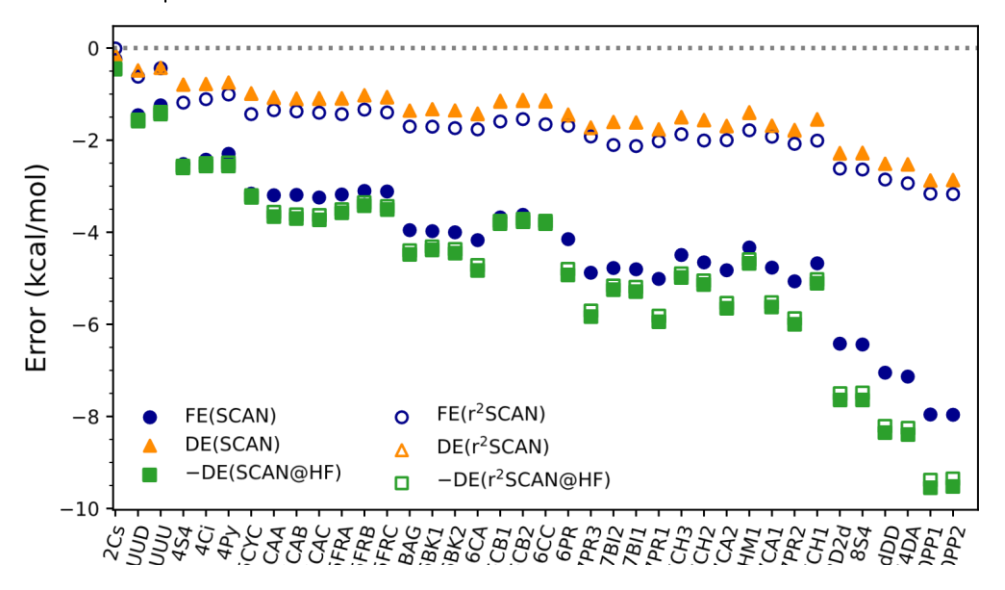


FIG. 1. Functional-driven errors (FEs, blue circles), density driven errors (DEs) for DFA (orange triangles), and for DFA@HF (green squares) for SCAN (closed symbols) and r²SCAN (open symbols) on the BEGDB set of neutral water clusters. All units are kcal/mol. The SCAN and r²SCAN DEs almost coincide, as do those of SCAN@HF and r²SCAN@HF. SCAN makes substantially larger FEs than r²SCAN, yielding the near perfect cancellation of FE and DE observed in SCAN@HF. As -DE(r²SCAN@HF)≪FE(r²SCAN), r²SCAN@HF underbinds the water clusters. Inclusion of a long-range dispersion correction, as in HF-r²SCAN-DC4 [14], eliminates the underbinding tendency.

for k optimized monomers. This makes intuitive sense and is the key to understanding HF-r<sup>2</sup>SCAN-DC4's accuracy for water clusters: the underbinding induced by evaluating r<sup>2</sup>SCAN on the HF density is almost perfectly eliminated by including a carefully-tuned dispersion correction. Moreover, r<sup>2</sup>SCAN may be a better candidate for a long-range dispersion correction,

energy and not its self-consistent density.

This near-perfect cancellation of errors in HF-r<sup>2</sup>SCANDC4 is made exceptionally clear in the water hexamer subset of BEGDB. The hexamers are the smallest clusters that realistically model monomer conformations in liquid water [13]. Thus an accurate description of primarily the relative

energy ordering of water hexamers is needed to realistically simulate liquid water. Fig. 2(a) shows that HF-SCAN-DC4 exceeds SCAN@HF's already exceptional accuracy for the absolute binding energies of the water hexamers (less than 0.8 kcal/mol in absolute error), as also shown in Ref. [14]. Fig. 2(b) plots the binding energies of the water hexamers rel-

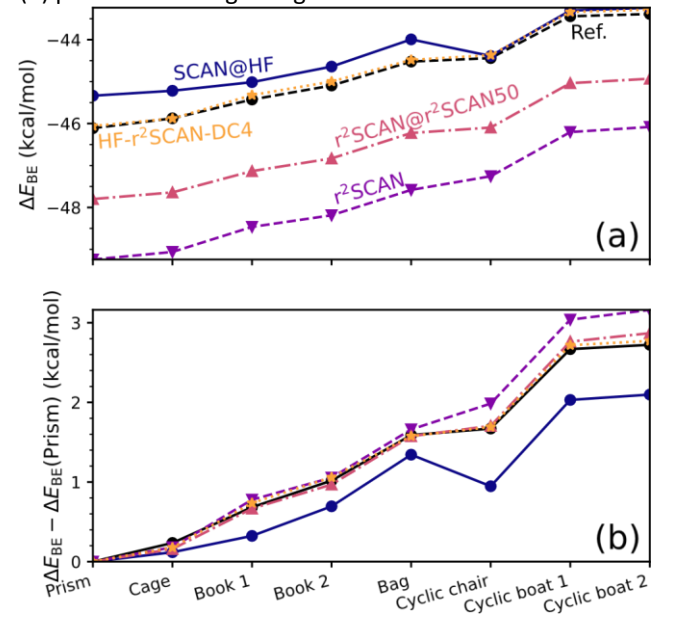


FIG. 2. (a) Absolute binding energies for the water hexamers in the BEGDB set. (b) Binding energies of the hexamers relative to the most stable isomer, the prism. While SCAN@HF (blue circles) is nearly chemically-accurate for the absolute binding energies of the hexamers, only HF-r<sup>2</sup>SCAN-DC4 is able to capture both properties with chemical accuracy. The composite method r<sup>2</sup>SCAN@r<sup>2</sup>SCAN50 eliminates the density errors of r<sup>2</sup>SCAN, but leaves a residual functional-driven error.

ative to the most stable isomer, the prism configuration. r²SCAN already predicts the relative binding energies of the hexamers with chemical accuracy. Applying r²SCAN to the r²SCAN50 density essentially eliminates its density errors, thereby making its relative energy ordering of the hexamers almost exact. The residual error in the absolute BEs from r²SCAN@r²SCAN50 are then purely functional-driven. HF-r²SCAN-DC4 again yields a chemically-accurate relative energy ordering. Note that SCAN@HF gives a wrong energy ordering for the hexamers, but all errors lie within a ±1 kcal/mol tolerance. Even without a correction, SCAN is reasonably good for liquid water, as shown in Ref. [32].

Very similar conclusions can be drawn from the neutral water cluster subset of the WATER27 dataset [19], as shown in Fig. 3 and Appendix Table V (analogous to Table I). The labeling schemes of Figs. 1 and 3 is identical to permit easy comparison. For the water dimer through to the octamer,  $FE(SCAN) \approx -DE(SCAN@HF)$ , whereas for the 20-mers, FE(SCAN) is markedly more negative than -DE(SCAN@HF).

For all these neutral clusters, FE( $r^2SCAN$ )  $\ll$  -DE( $r^2SCAN$ @HF), as before. Thus we can draw nearly identical conclusions: the improved description of intermediate-range dispersion interactions in SCAN permits SCAN@HF to make compensatory density- and functional-driven errors that describe small- to medium-sized water clusters.

Referring to the "Neutral" columns of Appendix Table V, this is made clear by looking at the changes in the mean FE and DE (MFE and MDE, respectively) from r<sup>2</sup>SCAN to r<sup>2</sup>SCAN@HF to HF-r<sup>2</sup>SCAN-DC4. Evaluating r<sup>2</sup>SCAN at the HF density increases its MDE to 8.4 kcal/mol from -2.6 kcal/mol, but leaves its -2.8 kcal/mol MFE unchanged. Adding a long-range dispersion correction to r<sup>2</sup>SCAN@HF, yielding HF-r<sup>2</sup>SCAN-DC4, significantly lowers the MFE to -8.6 kcal/mol, but leaves the MDE of r<sup>2</sup>SCAN@HF unchanged. Thus HF-r<sup>2</sup>SCAN-

DC4 benefits from a cancellation of relatively large errors.

However, in the 20-mers, long-range dispersion interactions become more important. We intuit this from markedly larger errors in the 20-mer binding energies from SCAN@HF, which cannot describe long-range dispersion interactions, than from HF-r<sup>2</sup>SCAN-DC4, which explicitly accounts for long-range dispersion.

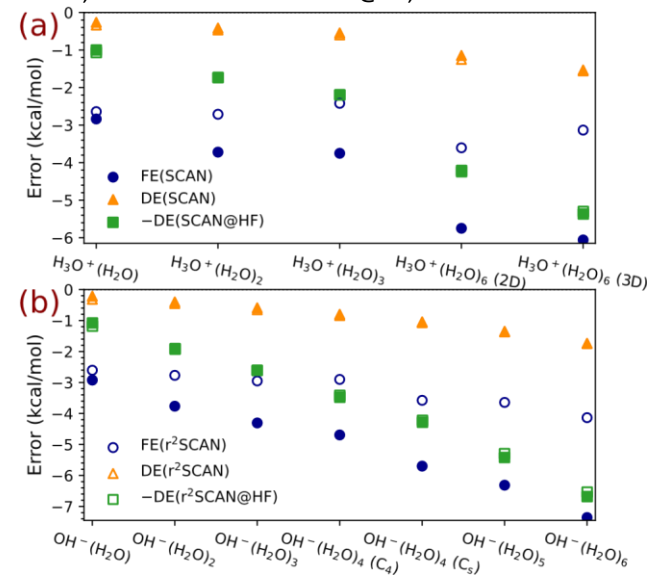
#### B. Charged water clusters

The remaining WATER27 dataset includes protonated, deprotonated, and autoionized water clusters. Fig. 4 presents the density- and functional-driven errors for the de/protonated water cluster subsets of WATER27, analogous to Fig. 3. For both subsets, it appears that SCAN overestimates the strength of the dispersion interaction between OH- or  $\rm H_3O^+$  and the induced multipole moments of the water clusters, yielding higher FEs than  $\rm r^2SCAN$  and which increase in magnitude monotonically with cluster size. Curiously, the  $\rm r^2SCAN$  FEs are mostly independent of the cluster size, and are about -3 kcal/mol from the monomer to the hexamer. The DEs of SCAN and  $\rm r^2SCAN$  are also mostly insensitive to the cluster size, whereas the DEs of SCAN@HF and  $\rm r^2SCAN$ @HF rise very quickly with cluster size.

The average errors presented in the "Protonated" and "Deprotonated" columns of Appendix Table V make it appear that r²SCAN@HF makes essentially no error for these clusters, with negative MFEs ( $\sim 3 \text{ kcal/mol}$ ) that cancel nearly perfectly with positive MDEs ( $\sim 3 - 3.6 \text{ kcal/mol}$ ). The dispersion correction in HF-r²SCANDC4 then vastly overcorrects r²SCAN@HF. However, referring back to Fig. 4 shows that this is true only in an average sense for the reasons mentioned in the previous paragraph.

The halide-water clusters have similar error patterns as the neutral and charged water clusters, whereas the alkali-water clusters have a notably different error pattern. Fig. 5(a) shows that  $\rm r^2SCAN's$  FEs for the alkaliwater clusters are strictly

positive. SCAN's FEs are positive only for Li<sup>+</sup>(H<sub>2</sub>O), Na<sup>+</sup>(H<sub>2</sub>O), K<sup>+</sup>(H<sub>2</sub>O), and Li<sup>+</sup>(H<sub>2</sub>O)<sub>2</sub>, and are smaller than r<sup>2</sup>SCAN's FEs. For Na<sup>+</sup>(H<sub>2</sub>O)<sub>2</sub> and K<sup>+</sup>(H<sub>2</sub>O)<sub>2</sub>, SCAN makes negative FEs that are larger in magnitude than r<sup>2</sup>SCAN's. The DEs of both SCAN and r<sup>2</sup>SCAN, either self-consistent or @HF,



are negligible for the alkali-water clusters, which makes intuitive sense, as these are closed-shell. However, because their DEs are negligible, SCAN@HF makes larger errors than for the neutral water clusters. The longrange dispersion correction in HF-r<sup>2</sup>SCAN-DC4 slightly reduces the tendency of r<sup>2</sup>SCAN@HF to underbind the alkali-water clusters, as shown in Appendix Table VI.

The DEs for the halide-water cluster set are notably larger than for the alkali-water clusters, which can be seen either from Fig. 5 or Appendix Table VI. In this case, the long-range dispersion correction of HF-r<sup>2</sup>SCANDC4 causes it to systematically over-bind the clusters.

However, in both the alkali- and halide-water cluster cases, the actual scales of the errors are tiny compared to the BEGDB and WATER27 sets: All DFAs considered here make absolute errors between 0 and 2 kcal/mol for these sets. Indeed, all predict the alkali-water cluster binding energies with chemical accuracy, and all but SCAN and r<sup>2</sup>SCAN predict the halide-water cluster binding energies with chemical accuracy, as seen in Appendix Table VI.

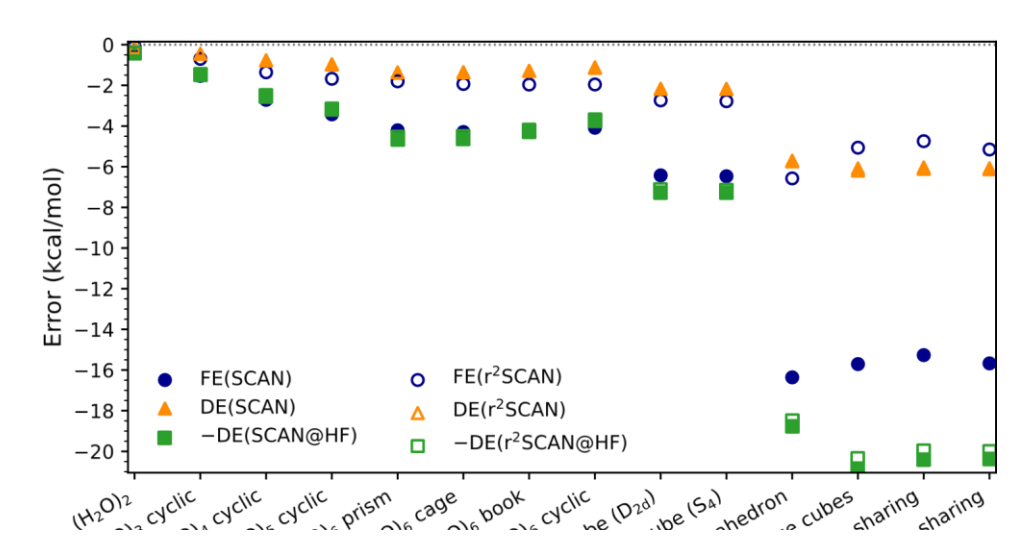
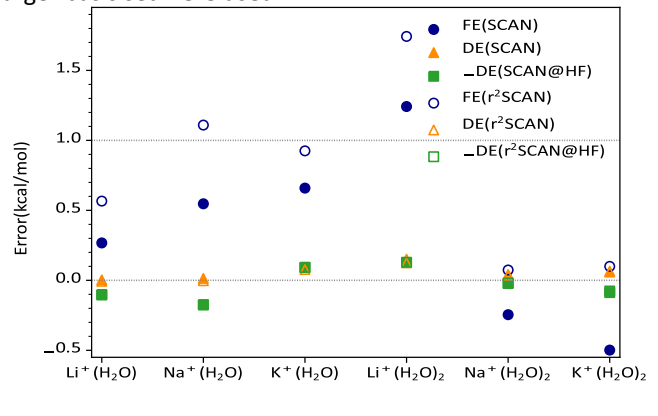


FIG. 3. Functional-driven errors (FEs, blue circles) and density-driven errors (DEs, orange triangles) for SCAN (closed symbols) and r<sup>2</sup>SCAN (open symbols) on the neutral-cluster subset of the WATER27 dataset [19] Negative DEs for DFA@HF are shown as green squares. The cancellation between FE(SCAN) and DE(SCAN@HF) is nearly perfect for clusters up to the octamer, but is much less perfect for the 20-mers. In all cases, the r<sup>2</sup>SCAN50 density is used as a proxy for the exact density.

FIG. 4. Functional-driven errors (blue circles) and densitydriven errors (orange triangles) for SCAN (closed symbols) and r<sup>2</sup>SCAN (open symbols) for the (a) protonated subset of WATER27, and for the (b) deprotonated subset of WATER27. Negative density-driven errors for DFA@HF are also shown as green squares.

As a further comparison to the work of Ref. [21], our FLOSIC results for SCAN and  $r^2SCAN$  are presented in Appendix Tables VII and VIII for the alkali- and halidewater clusters, respectively. By evaluating SCAN and  $r^2SCAN$  at their self-consistent FLOSIC densities, we find that FLOSIC offers no significant correction to the density of the alkali-water clusters. While we have found that the default NRLMOL basis

is insufficient for an accurate description of the halide-water cluster binding energies, our conclusions likely hold even if a larger basis set were used.



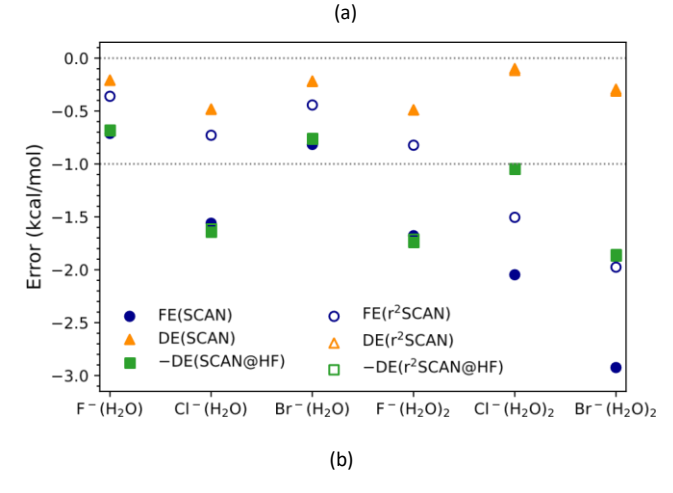


FIG. 5. Functional-driven errors (FEs, blue circles) and density-driven errors (DEs, orange triangles) for SCAN (closed symbols) and r<sup>2</sup>SCAN (open symbols). Negative DEs for SCAN@HF and r<sup>2</sup>SCAN@HF are shown as green squares.

Panel (a) plots these quantities for the alkali-water cluster set, and panel (b) for the halide-water cluster set.

# C. Comparison to barrier heights

Previous work by the authors and coworkers [6, 12] established similar patterns of error cancellation in DFA@HF for reaction barrier heights, and suggested that similar cancellation could be found for water clusters. While this has been borne out extensively in this work, the reason why the same patterns of error appear is not clear. Ref. [12] argued that there are two paradigms of FEs: stretched, symmetry-unbroken, neutral H<sub>2</sub>, where semi-local DFAs make large, positive FEs, and stretched H<sup>+</sup><sub>2</sub>, where they make large, negative FEs. Most of the BH76 transition states are stretched radicals, and none is like stretched H<sub>2</sub>, so the large negative FEs of the BH76 barrier heights are qualitatively explained. An independent analysis [33] of the BH76 reactions found (as did

Ref. [6]) that errors made by DFAs were in large-part due to delocalized orbitals in the stretched bonds of transition states. Residual errors due to the less-chemically-active orbitals were also significant in certain cases.

			W	ATER27	
DFA	вн76 ве	GDB	Neutral P	rot. Dep	orot.
SCAN	119.90	11.78	10.41	6.89	8.21
SCAN@HF	41.22	1.22	2.45	2.59	2.56
r <sup>2</sup> SCAN	107.42	6.67	6.88	5.30	6.12
r <sup>2</sup> SCAN@HF	42.35	6.13	4.38	1.82	1.82

TABLE II. Mean absolute percentage errors (MAPEs) in the reaction barrier heights from Ref. [6], the BEGDB neutral water cluster binding energies, and the binding energies of the WATER27 subsets. The WATER27 set includes neutral, protonated (Prot.), and deprotonated (Deprot.) clusters.

We find, but have no qualitative explanation for, negative FEs in the water-cluster binding energies (which also seem to be self-interaction errors [21, 34]). These are neither like  $H^+_2$  nor like  $H_2$ , in that the water clusters dissociate to purely closed-shell fragments. Instead, we note that SCAN and  $r^2$ SCAN predict the binding energies of the water dimer with chemical accuracy, and that their errors grow monotonically with cluster size. Indeed, any numerical method, including full configuration interaction, will make errors that become infinite in the thermodynamic limit. By considering mean absolute percentage errors (MAPEs),

$$PE = (100\%) \times \underline{EDFA - Eexact}, \qquad (12)$$

$$E_{exact}$$

in Table II, one sees immediately that the scales of relative errors for any of the water clusters and the barrier heights are completely different. The BH76 MAPEs of SCAN and r<sup>2</sup>SCAN are 120% and 110%, respectively, whereas for BEGDB, they are 12% and 7%, respectively. The much smaller relative errors of the water cluster binding energies are not amenable to qualitative explanation. Appendix Figs. 7(a) and 8(a) suggest that the percentage errors of any of the methods used here saturate to a constant value with cluster size. This constant value reflects the nature of an approximation: lack of manybody dispersion, self-interaction errors, etc. The modest relative overestimation of binding energies by SCAN or r<sup>2</sup>SCAN would presumably lead to a modest overestimation of boiling temperatures.

Appendix Fig. 7 shows that the relative errors of the binding energies are almost saturated at the quadramer (four water molecules), suggesting that all errors are local. Table II of Ref. [12] showed, by Kohn-Sham inversion of the CCSD(T) density, that r<sup>2</sup>SCAN50 is an almost-perfect proxy for the exact density in the evaluation of our Eqs. (6) and (11) for the binding energy of the water dimer. In the present work, we have taken the r<sup>2</sup>SCAN50 density as a proxy for the exact

density in all water clusters. When it becomes possible to make an accurate Kohn-Sham inversion of the CCSD(T) density for the water trimer and quadramer, this choice of a proxy-exact density could be strongly confirmed or disconfirmed.

Another possible metric that saturates under increasing system size is the error per hydrogen bond (HBE),

To determine the number of hydrogen bonds  $N_{\rm HB}$ , we use a bond indicator suggested by Ref. [35]. Any finite system in Kohn-Sham theory has a turning surface of its Kohn-Sham potential. For an atom, the turning surface is perfectly spherical; e.g., the turning surface radii for oxygen and hydrogen are  $R_0 = 1.13$  Å and  $R_{\rm H} = 1.06$  Å, respectively. Suppose nuclei A and B are separated by a distance  $s_{\rm AB}$  in a molecule. Then Ref. [35] proposed using the dimensionless quantity

$$\beta_{AB} = \frac{SAB}{R_A + R_B}$$
 (14)

to characterize covalent bonding  $\beta_{AB} \lesssim 0.7$ , hydrogen bonding  $0.7 \lesssim \beta_{AB} \lesssim 0.9$ , ionic bonding  $0.9 \lesssim \beta_{AB} \lesssim 1.3$ , and van der Waals bonding  $1.3 \lesssim \beta_{AB}$ . Then for any given molecular structure, we count the number of unique pairs of nuclei A and B that satisfy  $0.7 \leq \beta_{AB} \leq 0.9$ , and call this the approximate number of hydrogen bonds in the molecule  $N_{HB}$ . Appendix Figs. 7(b) and 8(b) show that these errors also saturate as a function of cluster size.

## IV. CONCLUSIONS

The present work seeks to understand the remarkable accuracy of water cluster binding energies predicted by the SCAN and r<sup>2</sup>SCAN meta-GGAs evaluated non-selfconsistently on the Hartree-Fock (HF) density. To do this, we use approximate measures of functional-driven errors (FEs) and density-driven errors (DEs) established by Ref. [6] to study the same errors in reaction barrier heights. For the water dimer, Ref. [12] demonstrated that approximate FEs and DEs in its binding energy computed with the 50% global hybrid of r<sup>2</sup>SCAN (r<sup>2</sup>SCAN50) were less than 0.1 kcal/mol in error. Thus we use the r<sup>2</sup>SCAN50 density as a proxy for the unavailable, exact Kohn-Sham density.

We have shown that the improved description of intermediate-range van der Waals interactions in SCAN, over r<sup>2</sup>SCAN, tends to cause it to overestimate the strength of these interactions in small water clusters. This yields more negative FEs for SCAN than for r<sup>2</sup>SCAN for neutral water

clusters. Consistent with the development of the D-series of dispersion corrections, inclusion of a greater fraction of dispersion interactions alters primarily the energy and not the density in a selfconsistent calculation. Thus SCAN and  $\rm r^2SCAN$  (or both evaluated at the HF density) yield nearly identical DEs. However,  $\rm -DE(SCAN@HF) \approx FE(SCAN@HF)$ , permitting an essentially perfect cancellation of large FE and DE. Because  $\rm r^2SCAN@HF$  tends to underbind water clusters, incorporating a tuned D4 [14, 30] dispersion correction to  $\rm r^2SCAN@HF$  almost completely eliminates this underbinding tendency. These conclusions are consistent for the neutral water clusters in the BEGDB [15]

and WATER27 [19] data sets. Thus we are able to understand why the composite methods SCAN@HF and HFr<sup>2</sup>SCAN-DC4 achieve chemical accuracy for many water clusters.

Note that r<sup>2</sup>SCAN alone is chemically exact for the relative energy ordering of the water hexamer binding energies (BEs). These have been argued to be relevant for an accurate description of liquid water. Evaluating r<sup>2</sup>SCAN on its 50% global hybrid density essentially eliminates its density-driven errors, and makes its description of the relative BE ordering exact. Thus any residual errors in the r<sup>2</sup>SCAN@r<sup>2</sup>SCAN50 absolute binding energies are purely functional-driven, and may be corrected with an explicit dispersion correction. We confirm the finding of Ref. [14] that HF-r<sup>2</sup>SCAN-DC4 is chemically exact for both the absolute and relative energy ordering of the water hexamer binding energies.

For charged water clusters, and for charged alkali- or halide-water clusters, the role of dispersion interactions with induced multipole moments becomes more important than for the neutral clusters. However, we are able to draw similar conclusions as for the neutral clusters. An improved description of monopole-multipole moments might permit more accurate predictions of these sets of water clusters.

Unlike the set of reaction barriers (the BH76 set [19]) considered in Ref. [6], the set of water clusters has no stretched bond. Ref. [12] argued that none of the transition states in BH76 were like stretched H2, where DFAs make large positive FEs, and were closer to the stretched radical bonding characteristic of stretched  $H^{+}_{2}$ , where DFAs make large negative FEs. However, by observing that the relative errors, either conventional percentage errors or the absolute error per hydrogen bond, made by DFAs converge to a (nearly) constant value with respect to cluster size, we can intuit that we are simply observing the effect of approaching the thermodynamic limit: any numerical method makes infinite errors in the limit of infinite particles.

Further validation of r<sup>2</sup>SCAN50 as a proxy for the exact density in water clusters would perform Kohn-Sham inversion of the exact density in water tetramers and quadramers. It is not currently possible to do this to numeric precision sufficient for assessing the relatively small errors in the binding energies of water clusters much bigger than the dimer.

For molecular properties and for semilocal DFAs, Hartree-Fock DFT or DFA@HF makes errors that are typically either comparable to, or much smaller than, those of self-consistent DFA [36]. Thus the unconventional error cancellation in DFA@HF between FE and DE seems to be rather reliable Ref. [12] used a figure to explain this reliability, but we will here make the argument with words alone. The first key fact is that the exact density falls between the DFA density and the HF density on a localization scale (as shown for the water dimer in Ref. [4]). The energy of each functional is quadratic or parabolic under small variations around its own density. Thus the density-driven error defined by Eq. (11) can be much larger in magnitude than the one defined by Eq. (4). More relevantly, the exact functional evaluated on the HF density can be close in energy to the exact functional evaluated on the exact density. The second key fact is that an approximate density functional is closer [37] to the exact functional for the localized or integerpreferring (Fig. 3 of Ref. [2]) HF density than for its own self-consistent density. Thus the exact functional on the exact density can be close to the exact functional on the HF density, which, in turn, can be close to a good DFA like SCAN or r<sup>2</sup>SCAN evaluated on the HF density. Wherever there is the possibility of a charge-transfer error in self-consistent DFA, there may be a likelihood of improved energetics from DFA@HF.

Future work might attempt to extend this analysis or methods like SCAN@HF or HF-r<sup>2</sup>SCAN-DC4 to solids.

Delocalization errors likely plague calculations of transition metal monoxides and point defects (where selfinteraction errors in particular are expected to be important). However, HF calculations in solids are often impractical, especially for the sizes needed to study point defects. Thus one would need to find a computationally tractable method that yields highly-localized densities, and retune the dispersion correction to yield a comparably accurate composite method for solids.

#### **ACKNOWLEDGMENTS**

A.D.K. thanks Temple University for a Presidential Fellowship, and the US Department of Energy, Office of Science, Office of Basic Energy Sciences, Materials Sciences and Engineering Division, under contract no. DE-ACO2-05-CH11231 (Materials Project program KC23MP). C.S. and J.P.P. were supported by the U.S. Department of Energy, Office of Science, Office of Basic Energy Sciences, as part of the Computational Chemical Sciences Program, under Award No. DE-SC0018331. R.K.S., P.B., and J.P.P. were supported by National Science Foundation (NSF) grant DMR-1939528. This research includes calculations carried out on HPC resources supported in part by the NSF through major research instrumentation grants, numbers 1625061 and 2216289, and by the U.S. Army Research Laboratory under contract number W911NF-16-2-0189.

- [1] J. P. Perdew, R. G. Parr, M. Levy, and J. L. Balduz Jr., Phys. Rev. Lett. 49, 1691 (1982).
- [2] P. Mori-Sánchez, A. J. Cohen, and W. Yang, Phys. Rev. Lett. 100, 146401 (2008).
- [3] J. P. Perdew and A. Zunger, Phys. Rev. B 23, 5048 (1981).
- [4] S. Dasgupta, C. Shahi, P. Bhetwal, J. P. Perdew, and F. Paesani, J. Chem. Theory Comput. 18, 4745 (2022).
- [5] J. Sun, A. Ruzsinszky, and J. P. Perdew, Phys. Rev. Lett. 115, 036402 (2015).
- [6] A. D. Kaplan, C. Shahi, P. Bhetwal, R. K. Sah, and J. P. Perdew, J. Chem. Theory Comput. 19, 532 (2023). [7] M.-C. Kim, E. Sim, and K. Burke, Phys. Rev. Lett. 111, 073003 (2013).
- [8] A. Wasserman, J. Nafziger, K. Jiang, M.-C. Kim, E. Sim, and K. Burke, Annu. Rev. Phys. Chem. 68, 555 (2017). [9] E. Sim, S. Song, and K. Burke, J. Phys. Chem. Lett. 9, 6385 (2018).
- [10] S. Vuckovic, S. Song, J. Kozlowski, E. Sim, and K. Burke, J. Chem. Theory Comput. 15, 6636 (2019).
- [11] Y. Kim, S. Song, E. Sim, and K. Burke, J. Phys. Chem. Lett. 10, 295 (2019).
- [12] B. Kanungo, A. D. Kaplan, C. Shahi, V. Gavini, and J. P. Perdew, J. Phys. Chem. Lett. 15, 323 (2024).
- [13] S. Dasgupta, E. Lambros, J. Perdew, and F. Paesani, Nature Commun. 12, 6359 (2021).
- [14] S. Song, S. Vuckovic, Y. Kim, H. Yu, E. Sim, and K. Burke, Nat. Commun. 14, 799 (2023).

- [15] J. Řezáč, P. Jurečka, K. E. Riley, J. Černý, H. Valdes, K. Pluháčková, K. Berka, T. Řezáč, M. Pitoňák, J. Vondrášek, and P. Hobza, Collec. Czech. Chem. Commun. 73, 1261 (2008).
- [16] V. S. Bryantsev, M. S. Diallo, A. C. T. van Duin, and W. A. Goddard, J. Chem. Theory Comput. 5, 1016 (2009).
- [17] B. Temelso, K. A. Archer, and G. C. Shields, J. Phys. Chem. A 115, 12034 (2011).
- [18] D. Manna, M. K. Kesharwani, N. Sylvetsky, and J. M. L. Martin, J. Chem. Theory Comput. 13, 3136 (2017).
- [19] L. Goerigk, A. Hansen, C. Bauer, S. Ehrlich, A. Najibi, and S. Grimme, Phys. Chem. Chem. Phys. 19, 32184 (2017), and website http://www.thch.uni-bonn.de/tc. old/downloads/GMTKN/GMTKN55/BH76.html.
- [20] T. H. Dunning, J. Chem. Phys. 90, 1007 (1989).
- [21] K. Wagle, B. Santra, P. Bhattarai, C. Shahi, M. R. Pederson, K. A. Jackson, and J. P. Perdew, J. Chem. Phys. 154, 094302 (2021).
- [22] F. Weigend, F. Furche, and R. Ahlrichs, J. Chem. Phys. 119, 12753 (2003).
- [23] F. Weigend and R. Ahlrichs, Phys. Chem. Chem. Phys. 7, 3297 (2005).
- [24] D. Rappoport and F. Furche, J. Chem. Phys. 133, 134105 (2010).
- [25] Q. Sun, J. Comput. Chem. 36, 1664 (2015).
- [26] Q. Sun, T. C. Berkelbach, N. S. Blunt, G. H. Booth,

- S. Guo, Z. Li, J. Liu, J. D. McClain, E. R. Sayfutyarova, S. Sharma, S. Wouters, and G. K.-L. Chan, WIREs Comput. Mol. Sci. 8, e1340 (2018).
- [27] Q. Sun, X. Zhang, S. Banerjee, P. Bao, M. Barbry, N. S. Blunt, N. A. Bogdanov, G. H. Booth, J. Chen, Z.-H. Cui, J. J. Eriksen, Y. Gao, S. Guo, J. Hermann, M. R. Hermes, K. Koh, P. Koval, S. Lehtola, Z. Li, J. Liu, N. Mardirossian, J. D. McClain, M. Motta, B. Mussard, H. Q. Pham, A. Pulkin, W. Purwanto, P. J. Robinson, E. Ronca, E. R. Sayfutyarova, M. Scheurer, H. F. Schurkus, J. E. T. Smith, C. Sun, S.-N. Sun, S. Upadhyay, L. K. Wagner, X. Wang, A. White, J. D. Whitfield, M. J. Williamson, S. Wouters, J. Yang, J. M. Yu, T. Zhu, T. C. Berkelbach, S. Sharma, A. Y. Sokolov, and G. K.-L. Chan, J. Chem. Phys. 153, 024109 (2020).
- [28] J. W. Furness, A. D. Kaplan, J. Ning, J. P. Perdew, and J. Sun, J. Phys. Chem. Lett. 11, 8208 (2020), correction, *ibid*. 11, 9248 (2020).
- [29] (2022), R. R. Zope, T. Baruah, Y. Yamamoto, L. Basurto, C. Diaz, J. Peralta, and K. A. Jackson, FLOSIC 0.1.2, based on the NRLMOL Code of M. R. Pederson.
- [30] E. Caldeweyher, S. Ehlert, A. Hansen, H. Neugebauer, S. Spicher, C. Bannwarth, and S. Grimme, The Journal of Chemical Physics 150, 154122 (2019).
- [31] J. Ning, M. Kothakonda, J. W. Furness, A. D. Kaplan, S. Ehlert, J. G. Brandenburg, J. P. Perdew, and J. Sun, Phys. Rev. B 106, 075422 (2022).

- [32] M. Chen, H.-Y. Ko, R. C. Remsing, M. F. C. Andrade, B. Santra, Z. Sun, A. Selloni, R. Car, M. L. Klein, J. P. Perdew, and X. Wu, Proc. Natl. Acad. Sci. U.S.A. 114, 10846 (2017).
- [33] P. B. Shukla, P. Mishra, T. Baruah, R. R. Zope, K. A. Jackson, and J. K. Johnson, J. Phys. Chem. A 127, 1750 (2023).
- [34] K. Sharkas, K. Wagle, B. Santra, S. Akter, R. R. Zope, T. Baruah, K. A. Jackson, J. P. Perdew, and J. E. Peralta, Proc. Natl. Acad. Sci. U.S.A. 117, 11283 (2020).
- [35] E. Ospadov, J. Tao, V. N. Staroverov, and J. P. Perdew, Proc. Nat. Acad. Sci. U.S.A. 115, E11578 (2018).
- [36] G. Santra and J. M. Martin, J. Chem. Theory Comput. 17, 1368 (2021).
- [37] J. P. Perdew, Density functional methods in physics (Plenum, 1985) pp. 265–308.
- [38] D. Porezag and M. R. Pederson, Phys. Rev. A 60, 2840 (1999).
- [39] B. P. Pritchard, D. Altarawy, B. Didier, T. D. Gibson, and T. L. Windus, J. Chem. Inf. Model. 59, 4814 (2019). [40] D. Feller, J. Comput. Chem. 17, 1571 (1996).
- [41] K. L. Schuchardt, B. T. Didier, T. Elsethagen, L. Sun, V. Gurumoorthi, J. Chase, J. Li, and T. L. Windus, J. Chem. Inf. Model. 47, 1045 (2007).

Appendix A: Basis set dependence of the alkali- and halide-water cluster binding energies

Tables III and IV present the binding energies and their errors for the alkali- and halide-water clusters, respectively, as computed with three different basis sets: the standard NRLMOL basis set [38], the NRLMOL basis set augmented with diffuse functions [21], and with the much larger def2-QZVPPD basis set [24]. The NLRMOL basis set was taken from the Basis Set Exchange [39–41]. While the alkali-water clusters are relatively insensitive to the basis set choice, the halide-water clusters are highly sensitive to the basis set. The differences are highly significant, differing on the order of kcal/mol.

Although we do not show the calculations here, the halide-water cluster binding energies computed with def2QZVPPD are comparable to those computed with the aug-cc-pV5Z basis set [20]. Differences in the binding energies computed with these basis sets are on the order of tenths of kcal/mol.

		LSDA			PBE			SCAN		
	Reference	Ref. [21] NRLI	MOL	def2-	Ref. [21] NRLN	MOL	def2-	Ref. [21] NRLI	MOL	def2-
			QZ	VPPD		QZ	VPPD		Q	ZVPPD
K+H2O	-17.96	-2.03	-2.00	-2.29	1.10	1.07	0.80	0.39	0.45	0.27
K+(H2O)2	-33.85	-3.69	-3.64	-4.04	2.07	2.03	1.66	0.74	0.81	0.56
Li+H <sub>2</sub> O	-34.78	-2.56	-2.44	-2.51	0.14	0.22	0.17	0.83	0.91	0.75
Li+(H <sub>2</sub> O) <sub>2</sub>	-64.75	-4.43	-4.31	-4.32	0.55	0.59	0.63	1.52	1.59	1.39
Na+H <sub>2</sub> O	-24.19	-2.56	-2.54	-2.40	0.32	0.31	0.38	-0.30	-0.27	-0.20
Na+(H2O)2	-45.80	-4.70	-4.67	-4.54	0.69	0.68	0.72	-0.46	-0.48	-0.43
MD		-3.33	-3.27	-3.35	0.81	0.82	0.73	0.45	0.50	0.39
MAD		3.33	3.27	3.35	0.81	0.82	0.73	0.71	0.75	0.60

TABLE III. Binding energies and their errors for the alkali-water clusters computed in Ref. [21] with the NRLMOL basis set [38] augmented with diffuse functions, here with the standard NLRMOL basis set, and here with the def2-QZVPPD [24] basis set.

LSDA	PBE	SCAN

	Reference	Ref. [21] NR	.MOL	def2-	Ref. [21] NR	LMOL	def2-	Ref. [21] NRL	MOL	def2-
				QZVPPD		QZ	VPPD		Q	ZVPPD
Br-H <sub>2</sub> O	-12.82	-5.28	-4.97	-4.31	-1.80	-1.46	-0.72	-1.57	-1.40	-0.92
Br-(H2O)2	-26.52	-11.02	-10.71	-9.61	-2.31	-1.96	-0.74	-3.00	-2.84	-2.04
CI-H <sub>2</sub> O	-14.87	-5.88	-5.51	-4.75	-1.96	-1.56	-0.73	-1.73	-1.56	-1.03
$CI^-(H_2O)_2$	-29.89	-11.67	-11.31	-10.09	-2.35	-1.97	-0.65	-3.18	-3.02	-2.17
F-H <sub>2</sub> O	-27.40	-10.58	-9.84	-7.94	-3.73	-2.92	-0.81	-4.10	-3.64	-2.15
F-(H <sub>2</sub> O) <sub>2</sub>	-48.70	-15.78	-15.29	-12.75	-3.97	-3.46	-0.63	-5.45	-5.23	-3.22
MD		-10.04	-9.61	-8.24	-2.69	-2.22	-0.71	-3.17	-2.95	-1.92
MAD		10.04	9.61	8.24	2.69	2.22	0.71	3.17	2.95	1.92

TABLE IV. Binding energies and their errors for the halide-water clusters computed in Ref. [21] with the NRLMOL basis set [38] augmented with diffuse functions, here with the standard NLRMOL basis set, and here with the def2-QZVPPD [24] basis set.

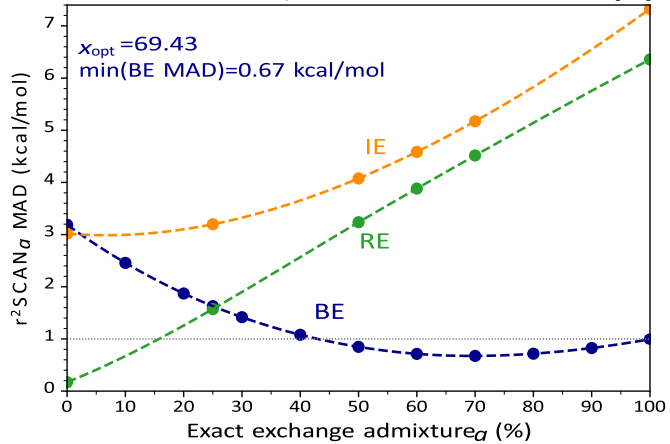


FIG. 6. Mean absolute deviations (MADs) in the binding energies (BEs), interaction energies (IEs), and relaxation energies (REs) for the neutral water cluster subset of BEGDB [15], plotted as a function of the fraction of exact exchange admixed into a global hybrid of r<sup>2</sup>SCAN. Although the BE MAD minimizes for about 70% exact exchange admixture, any global hybrid of r<sup>2</sup>SCAN with 50-100% exact exchange predicts chemically-accurate BEs. Importantly, Ref. [12] showed that the density of the 50% global hybrid of r<sup>2</sup>SCAN, r<sup>2</sup>SCAN50, is an excellent proxy for that of the exact density, at least for the water dimer. The REs rise almost linearly with the fraction of exact exchange mixture.

Appendix B: Auxiliary data for the water cluster sets

		Neutral		Protonated		Deprotonated		Total				
	MD	MAD MFE MDE		MDN	MAD MFE MDE		MDN	MAD MFE MDE		MDN	MAD MFE MDE	Ē
SCAN	-9.76	9.76 -7.19	-2.57	-5.20	5.20 -4.42	-0.78	-5.88	5.88 -5.01	-0.88	-7.25	7.86 -5.56	5 -1.68
SCAN@HF	1.38	1.48 -7.19	8.57	-1.53	1.53 -4.42	2.90	-1.38	1.38 -5.01	3.63	0.28	1.61 -5.56	5.84
r <sup>2</sup> SCAN	-5.30	5.30 -2.75	-2.55	-3.74	3.74 -2.90	-0.84	-4.14	4.14 -3.22	-0.92	-4.23	4.80 -2.54	-1.69
r <sup>2</sup> SCAN@HF	5.65	5.65 -2.75	8.40	-0.00	1.12 -2.90	2.90	0.36	1.12 -3.22	3.59	3.20	3.60 -2.54	5.74
HF-r <sup>2</sup> SCAN-DC4	-0.14	0.23 -8.55	8.40	-1.56	1.56 -4.46	2.90	-1.71	1.71 -5.30	3.59	-0.65	1.01 -6.39	5.74
r <sup>2</sup> SCAN50	-2.19	2.19		-3.14	3.14		-3.24	3.24		-2.47	2.65	

TABLE V. Mean deviations (MDs), mean absolute deviations (MADs), mean functional-driven errors (MFEs), and mean density-driven errors (MDEs) for the subsets of the WATER27 set [19]. All units are kcal/mol. MFEs and MDEs are computed using  $r^2SCAN50$  as a proxy for the exact density only. By construction, MD = MFE + MDE. HF- $r^2SCAN$ -DC4 FEs and DEs are computed using the same method as in Table I.

		Alkali			Halide		
DFA	MDM	IAD MFE MDE		MD	MAD MFE MDE	Ĭ.	
SCAN	0.39	0.60 0.20	0.04	-1.92	1.92 -0.97	-0.18	
SCAN@HF	0.36	0.57 0.20	0.02	-0.33	0.38 -0.97	0.78	
r <sup>2</sup> SCAN	0.80	0.80 0.45	0.03	-1.28	1.28 -0.58	-0.18	
r <sup>2</sup> SCAN@HF	0.78	0.78 0.45	0.02	0.30	0.50 -0.58	0.77	
HF-r <sup>2</sup> SCAN-DC4	0.54	0.62 0.31	0.02	-0.29	0.29 -0.94	0.77	
r <sup>2</sup> SCAN50	-0.83	0.83		-0.49	0.58		

TABLE VI. Same as Table V, but for the binding energies of the charged alkali and halide water clusters considered here [21].

System	Ref. SCAN@FLOSIC SCAN-FLOSIC r <sup>2</sup> SCAN@FLOSIC r <sup>2</sup> SCAN-FLOSIC								
$K^+(H_2O)$	-17.96	0.16	-0.44	0.45	0.49				
K+(H2O)2	-33.85	0.34	-0.15	0.92	1.64				
Li <sup>+</sup> (H <sub>2</sub> O)	-34.78	0.62	-0.62	0.87	-0.35				
$Li^+(H_2O)_2$	-64.75	1.06	-1.24	1.52	-0.56				
Na+(H <sub>2</sub> O)	-24.19	-0.50	-1.58	-0.15	-0.83				
Na+(H <sub>2</sub> O) <sub>2</sub>	-45.80	-0.88	-3.02	-0.22	-0.51				
	MD	0.14	-1.17	0.57	-0.02				
	MAD	0.59	1.17	0.69	0.73				
	MAPE	1.55	3.28	1.86	2.33				

TABLE VII. Individual errors for the alkali-water cluster set considered here, for DFA-FLOSIC, DFA@DFA-FLOSIC (DFA@FLOSIC), where DFA = SCAN, r<sup>2</sup>SCAN. All units are kcal/mol. Reference (Ref.) values are taken from Ref. [21]. Mean deviations (MDs), mean absolute deviations (MADs), and mean absolute percentage errors (MAPEs) are presented in the final three rows. All calculations used the NLRMOL basis set [38].

System	Ref. SCAN@FLOSIC SCAN-FLOSIC r <sup>2</sup> SCAN@FLOSIC r <sup>2</sup> SCAN-FLOSIC							
$Br^{-}(H_2O)$	-12.82	-0.98	0.45	-0.59	1.52			
$Br^{-}(H_{2}O)_{2}$	-26.52	-2.61	-1.73	-1.70	0.29			
CI-(H <sub>2</sub> O)	-14.87	-1.16	0.30	-0.75	1.27			
$CI^{-}(H_{2}O)_{2}$	-29.89	-2.95	-2.36	-1.95	-0.36			
F-(H <sub>2</sub> O)	-27.40	-3.71	-3.42	-3.16	-2.32			

F-(H <sub>2</sub> O) <sub>2</sub>	-48.70	-5.32	-5.48	-4.31	-2.95
	MD	-2.79	-2.04	-2.08	-0.43
	MAD	2.79	2.29	2.08	1.45
	MAPE	9.94	7.30	7.15	6.20

TABLE VIII. Same as Table VII, but for the set of halide-water clusters.

Appendix C: Relative error analysis

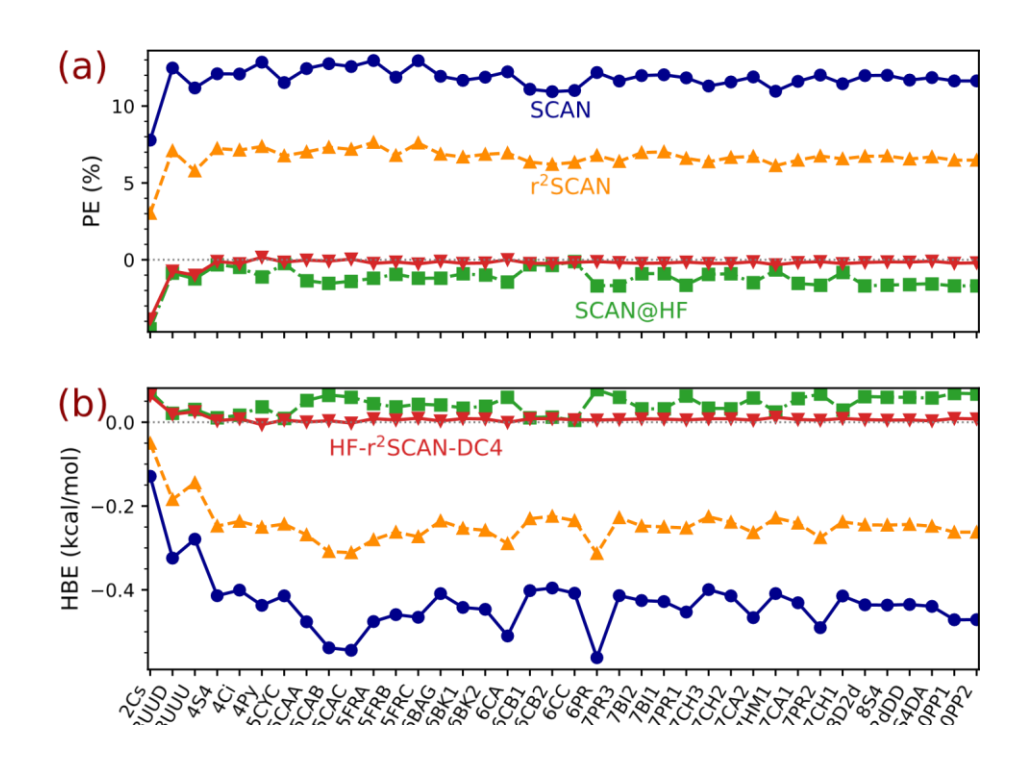


FIG. 7. (a) Percentage errors (PEs) in the binding energies of the water clusters of the BEGDB set. (b) Errors per hydrogen bond (HBEs), in units of kcal/mol, for the same set. In both cases, the relative errors appear to saturate to constant values as the size of the clusters increase.

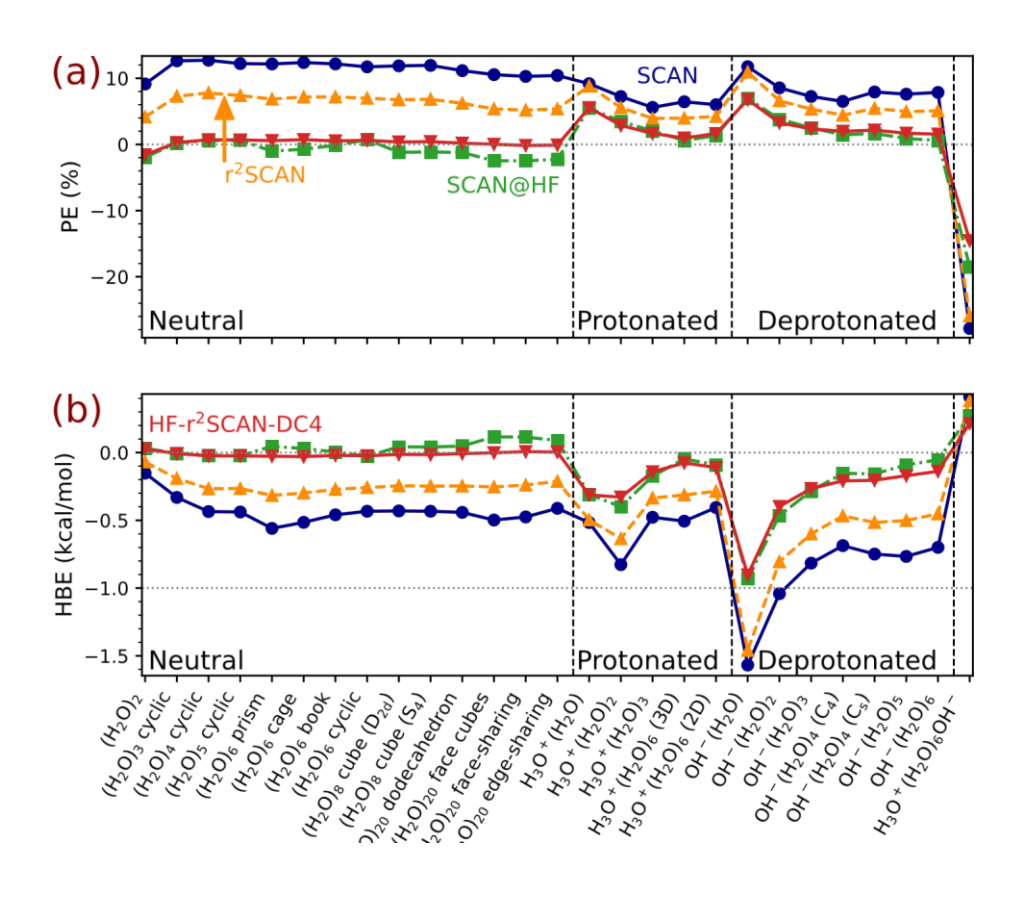


FIG. 8. Same as Fig. 7, but for the WATER27 set and its three primary subsets: neutral, protonated, and deprotonated clusters. The autoionized water octamer,  $H_3O^+(H_2O)_6OH^-$ , is located at the rightmost tick. Although overall neutral, the presence of two oppositely charged species,  $H_3O^+$  and  $OH^-$ , is expected to induce multipole moments that would not be observed in the neutral water clusters.